VI-G Photoionization and Photodissociation Dynamics Studied by Electron and Fluorescence Spectroscopy

Molecular photoionization is a major phenomenon in vacuum UV excitation and provides a large amount of information on fundamental electron-core interactions in molecules. Especially, neutral resonance states become of main interest, since they often dominate photoabsorption cross sections and lead to various vibronic states which are inaccessible in direct ionization. We have developed a versatile machine for two-dimensional photoelectron spectroscopy in order to elucidate dynamical aspects of superexcited states such as autoionization, resonance Auger decay, predissociation, vibronic couplings, and internal conversion. In a two-dimensional photoelectron spectrum (2D-PES), the photoelectron yield is measured as a function of both photon energy $E_{h\nu}$ and electron kinetic energy E_k (binding energy). The spectrum, usually represented as a contour plot, contains rich information on photoionization dynamics.

Photofragmentation into ionic and/or neutral species is also one of the most important phenomena in the vacuum UV excitation. In some cases, the fragments possess sufficient internal energy to de-excite radiatively by emitting UV or visible fluorescence. It is widely accepted that fluorescence spectroscopy is an important tool to determine the fragments and to clarify the mechanisms governing the dissociation processes of diatomic and polyatomic molecules. For several years we have concentrated our energies on fluorescence spectroscopy of H_2O in the photon energy region of 15–55 eV.

VI-G-1 Photofragmentaion Mechanisms of H_2O Studied by Ultraviolet Dispersed Spectroscopy

MITSUKE, Koichiro

[*J. Electron Spectrosc. Relat. Phenom.* submitted]

Fragmentation of H_2O has been studied by dispersed fluorescence spectroscopy at excitation photon energies above 20 eV. Figure 1 shows expanded dispersed spectra in the wavelength range from 280 to 420 nm. With appearance energies of $h\nu \sim 30$ eV several vibrational bands, marked with diamond symbols, begin to emerge below 320 nm. We have assigned these peaks to $OH(A^2\Sigma^+ \rightarrow X\ ^2\Pi)$ transition, judging from characteristic peaks due to the R_1 band heads for the $\Delta v = v' - v'' = 0$ sequence at 306.4, 312.6, and 318.8 nm. The counter fragment of $OH(A^2\Sigma^+)$ must be $H^*(n)$ in the Rydberg state with $n \geq 2$. The above appearance energies are much higher than the dissociation limits for the OH $(A^2\Sigma^+)$ + $H^*(n \geq 2)$ channels, but in good agreement with the vertical transition energies[2] for the associated Rydberg states of H_2O.

References

1) K. Mitsuke, *J. Chem. Phys.* **117**, 8334–8340 (2002).
2) J. Appell and J. Durup, *Int. J. Mass Spectrom. Ion Phys.* **10**, 247–265 (1972/73).

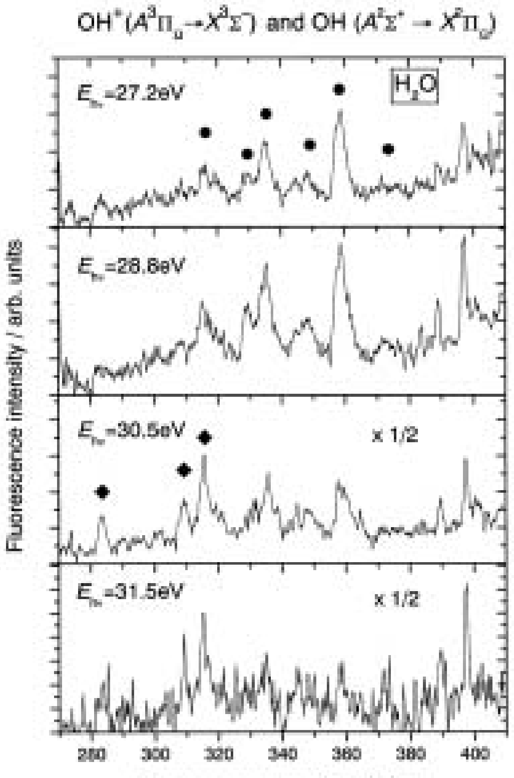

Figure 1. Dispersed fluorescence spectra of H_2O. The symbols ● and ◆ designate the vibrational bands due to the $OH^+(A^3\Pi \rightarrow X\ ^3\Sigma^-)$ and $OH(A\ ^2\Sigma^+ \rightarrow X\ ^2\Pi)$ transitions, respectively.

VI-G-2 Autoionization and Neutral Dissociation of Superexcited HI Studied by Two-Dimensional Photoelectron Spectroscopy

HIKOSAKA, Yasumasa; MITSUKE, Koichiro

[*J. Chem. Phys.* **121**, 792–799 (2004)]

Two-dimensional photoelectron spectroscopy of hydrogen iodide HI has been performed in the photon energy region of 11.10–14.85 eV, in order to investigate dynamical properties on autoionization and neutral dissociation of Rydberg states HI*(R_A) converging to $HI^+(\tilde{A}\,^2\Sigma^+_{1/2})$. A two-dimensional photoelectron spectrum exhibits strong vibrational excitation of $HI^+(\tilde{X}\,^2\Pi)$ over a photon energy region from ~ 12 to 13.7 eV, which is attributable to autoionizing feature of the 5$d\pi$ HI*(R_A) state. A noticeable set of stripes in the photon energy region of 13.5–14.5 eV are assigned as resulting from autoionization of the atomic Rydberg states of I* converging to $I^+(^3P_0$ or $^3P_1)$. The formation of I* is understood in terms of predissociation of multiple HI*(R_A) states by way of the repulsive Rydberg potential curves converging to $HI^+(^4\Pi_{1/2})$.

VI-H Development of the Laser-SR Combination System for Photodissociation Studies of Highly Vibrationally Excited Molecules

Initial vibrational excitation in molecules might influence the chemical branching in photodissociation, if two or more different dissociation pathways are accessible from an electronically excited state. Much attention has been focused on the pioneering work of Crim and his collaborators [*J. Chem. Phys.* **92**, 803–805 (1990)], who could accomplish the selective bond-breaking of heavy water, HOD. Very recently Yokoyama, Akagi and coworkers reported that deuterized ammonia NHD_2 in the fourth N–H stretching overtone preferentially photodissociates into the ND_2 + H channel [*J. Chem. Phys.* **118**, 3600–3611 (2003)]. In these two studies UV lasers are employed for vibrationally mediated photodissociation.

Instead, we are planning to use synchrotron radiation (SR) to promote vibrationally excited molecules to electronically excited states in the vacuum UV region. The main objectives are as follows: (1) Elucidating the properties of dissociative states by sampling a wide range of their potential energy surfaces, such as dynamics determining the final-state distributions of the products, nonadiabatic transitions on dissociation, and assignments and characterization of unknown multiply-excited states produced by Auger decay from core-excited states. (2) Aiming at more universal “vibrational state-specific” rupture of chemical bonds, which could be realized by changing the overlap between the wavefucntions of the upper-state continuum and that of the ground state.

VI-H-1 Apparatus for Probing Dissociative Photoionization of Vibrationally Excited H_2O into $OH^+(X^3\Sigma^-)$ + H(n = 1)

MITSUKE, Koichiro; MORI, Takanori; KOU, Junkei; ADACHI, Junichi[1]; YAGISHITA, Akira[1]; AKAGI, Hiroshi[2]; YOYAMA, Atsushi[2]
(*[1]KEK-PF; [2]JAERI, Tokai)*

We have developed an experimental system for laser-SR two photon ionization the crux of which are an ultrahigh resolution continuous titanium-sapphire laser (a bandwidth of 4 × 10^{-4} cm^{-1}) and in-vacuum beam alignment devices for strict overlapping of the counter-propagating two photon beams. The apparatus was connected to the beam line 28A of the Photon Factory synchrotron radiation facility in Tsukuba. Figure 1 shows a schematic diagram of the experimental setup. The wavenumber of the laser was determined precisely in the range of from 13814 to 13819 cm^{-1} by observing photoacoustic signal from laser excited H_2O measured with a lock-in modulation technique. The photon beam alignment devices are situated upstream and downstream of a central photoionization chamber. Each device is comprised of two stainless steel plates fitted on two-dimensional motion feedthroughs individually adjustable: one plate has an aperture of 0.8 mmϕ and the other plate is coated with a fluorescing substance. These plates can be inserted across the photon beam axis without breaking the system vacuum, which permits us to easily attain good spatial overlap of the two beams. The OH^+ ions produced via dissociation of $H_2O^*(4\nu_{O-H}) + h\nu \rightarrow OH^+(X^3\Sigma^-) + H(n = 1) + e^-$ were detected by time-of-flight mass spectrometry at SR photon energies near the dissociation threshold of 18.05 eV with respect to the neutral ground state of water.

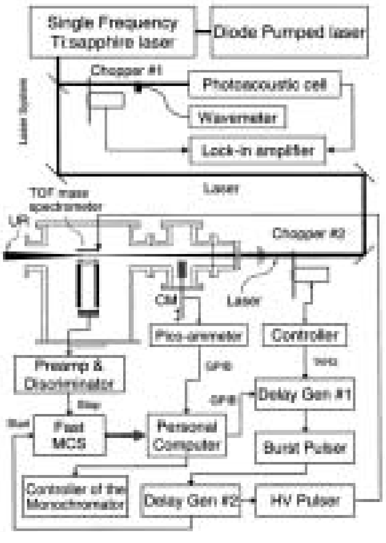

Figure 1. Schematic diagram of the setup for laser-SR two photon ionization experiments.

VI-I Extreme UV Photoionization Studies of Polyatomic Molecules and Fullerenes by Employing a Grazing-Incidence Monochromator

On the beam line BL2B2 in UVSOR a grazing incidence monochromator has been constructed which supplies photons in the energy region from 20 to 200 eV [M. Ono, H. Yoshida, H. Hattori and K. Mitsuke, *Nucl. Instrum. Methods Phys. Res., Sect. A* **467-468**, 577–580 (2001)]. This monochromator has bridged the energy gap between the beam lines BL3B and BL4B, thus providing for an accelerating demand for the high-resolution and high-flux photon beam from the research fields of photoexcitation of inner-valence electrons, *L*-shell electrons in the third-row atom, and 4*d* electrons of the lanthanides. Since 2001 we have measured photoion yield curves of fullerenes. Geometrical structures and electronic properties of fullerenes have attracted widespread attention because of their novel structures, novel reactivity, and novel catalytic behaviors as typical nanometer-size materials. Moreover, it has been emphasized that the potential for the development of fullerenes to superconductors (T_c ~ 50 K) and strong ferromagnetic substances is extremely high. In spite of such important species spectroscopic information is very limited in the extreme UV region, which has been probably due to difficulties in obtaining enough number density of the sample. The situation has been rapidly changed in these few years, since the techniques of syntheses, isolation, and purification have been advanced so rapidly that appreciable amount of fullerenes is obtainable from several distributors in Japan.

VI-I-1 Kinetic Energy Distribution and Anisotropy of Fragment Ions from SF_6 by Photoexcitation of a Sulfur 2p-Electron

ONO, Masaki[1]; MITSUKE, Koichiro
([1]Chiba Univ.)

[*Chem. Phys. Lett.* **379**, 248–254 (2003)]

The kinetic energy (KE) distribution and asymmetry parameter β have been studied for photofragmentation of SF_6 near the sulfur 2*p* ionization edges at 170–208 eV by using synchrotron radiation. The relative yield of fast ions with KE > 5 eV is larger in the post-edge than in the pre-edge region, whereas β of such ions is lower in the post-edge region. The β curve shows a sudden drop from 0.06–0.07 to zero near the edges and remains constant thereafter. These results are ascribed to *LVV* Auger decay occurring above the edges leading to SF_6^{2+} and SF_6^{3+} transiently. At KE > 2 eV the distribution curve for core excitation to the $(2t_{1u})^{-1}(6a_{1g})^1$ state resembles that for valence-electron ionization at 170 eV. This agreement, together with a similarity in β, suggests that the S 2p → $6a_{1g}$ resonance transition and valence-electron ionization undergo similar formation pathways leading to fast F^+ ions (*i.e.* participation of shake-up satellite states).

VI-I-2 Production of Doubly Charged Ions in Valence Photoionization of C_{60} and C_{70} at $h\nu$ = 25–150 eV

KOU, Junkei; MORI, Takanori; S. V. K. Kumar[1]; HARUYAMA, Yusuke[2]; KUBOZONO, Yoshihiro[3]; MITSUKE, Koichiro
([1]IMS and Tata Inst. Fund. Res.; [2]Okayama Univ.; [3]IMS and Okayama Univ.)

[*J. Chem. Phys.* **120**, 6005–6009 (2004)]

Photoion yields from gaseous fullerenes, C_{60} and C_{70}, for production of singly and doubly charged ions are measured by mass spectrometry combined with tunable synchrotron radiation at $h\nu$ = 25–150 eV. Since the signal of triply or highly charged ions is very weak, the total photoionization yield curve can be estimated from the sum of the yields of the singly and doubly charged ions. There is distinct disagreement between the resultant curve of C_{60} and the calculated total photoabsorption cross section previously reported. This difference is understood by the assumption that C_{60}^{2+} ions are chiefly produced by spectator Auger ionization of the shape resonance states followed by tunneling of the trapped electron or by cascade Auger ionization. For C_{60} and C_{70} the ratios between the yields of doubly and singly charged ions are larger than unity at $h\nu$ > 50 eV. These ratios are quite different from those reported in the experiments using electron impact ionization.

VI-I-3 Absolute Photoabsorption Cross Section of C_{60} in the Extreme Ultraviolet

MORI, Takanori; KOU, Junkei; HARUYAMA, Yusuke[1]; KUBOZONO, Yoshihiro[1]; MITSUKE, Koichiro
([1]Okayama Univ.)

[*J. Electron Spectrosc. Relat. Phenom.* submitted]

The absolute photoabsorption cross section curve of C_{60} has been determined by means of mass spectrometry with the photon source of monochromatized synchrotron radiation of $h\nu$ = 24.5–150 eV. Experiments are carried out using a high-temperature source of gaseous fullerenes and an efficient time-of-flight mass spectrometer. The absolute cross section curve is shown in Figure 1. The cross sections are 762, 241 and 195 Mb at $h\nu$ = 24.5, 90, and 110 eV, respectively with about 10% errors. Our results may suffer from some deviation from the real cross section curve. This deviation chiefly arises from uncertainties in the number density *n* of C_{60} in the ionization region, because we derive *n* from the mass deposition rate at the thickness monitor by assuming effusive flow conditions for the properties of the C_{60} beam. The present cross section curve was then normalized at $h\nu$ = 25 eV to the absolute cross section reported by Jaensch and Kamke,1) the most reliable data so far available in the valence region of C_{60}. Eventually, the present cross section data were reduced to 407, 144 and 114 Mb at $h\nu$ = 25, 90, and 110 eV, respectively.

References

1) R. Jaensch and W. Kamke, *Mol. Materials* **13**, 143–150 (2000).
2) J. Berkowitz, *J. Chem. Phys.* **111**, 1446–1453 (1999).

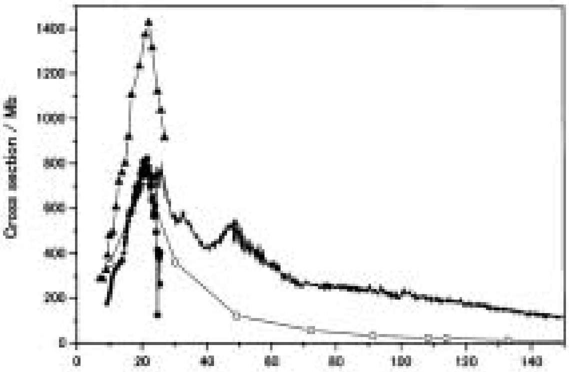

Figure 1. Absolute absorption cross section of C_{60} at $h\nu$ = 24.5–150 eV (solid line). The closed circles and triangles designate the data measured by Jaensch and Kamke1) and those compiled by Berkowitz,2) respectively. The open circles indicate the cross section of sixty carbon atoms.

VI-I-4 Photofragmentation of C_{60} in Valence Ionization

KOU, Junkei; MORI, Takanori; KUBOZONO, Yoshihiro[1]; MITSUKE, Koichiro
([1]Okayama Univ.)

[*J. Electron Spectrosc. Relat. Phenom.* submitted]

The yield curves for C_{60-2n}^+ (n = 1–3) produced by photoionization of C_{60} were measured in the $h\nu$ range of 25–150 eV. The appearance energies increase with increasing n, as evidenced from Figure 1. Evaluation was made on the upper limits of the internal energies of the primary C_{60}^+ above which $C_{60-2n+2}^+$ fragments ($n \geq 1$) cannot escape from further dissociating into C_{60-2n}^+ + C_2. These limits agree well with the theoretical internal energies of C_{60}^+ corresponding to the formation threshold for C_{60-2n}^+, assuming that the binding energies of $C_{60-2n+2}^+$ are equal to those proposed by Foltin *et al.*1)

Reference

1) M. Foltin, M. Lezius, P. Scheier and T. D. Märk, *J. Chem. Phys.* **98**, 9624–9634 (1993).

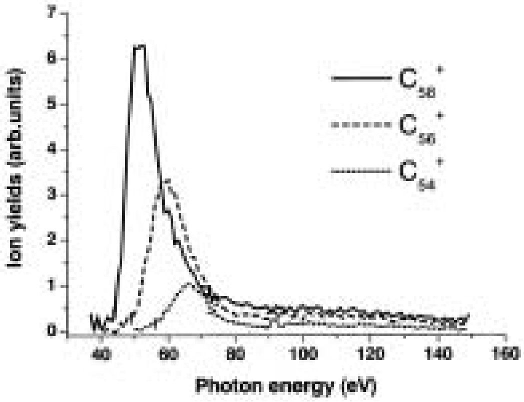

Figure 1. Yield curves for C_{60-2n}^+ ions (n = 1–3) obtained from time-of-flight mass spectra.

VI-I-5 Remarkably Large Shifts of the Appearance Energies of C_{60-2n}^{z+} ($n \geq 1$) from Their Thermochemical Thresholds

KOU, Junkei; MORI, Takanori; KUBOZONO, Yoshihiro[1]; MITSUKE, Koichiro
([1]Okayama Univ.)

[*Phys. Chem. Chem. Phys.* submitted]

The ion yield curves for C_{60-2n}^{z+} (n = 1–5, z = 1–3) produced by photoionizaiotion of C_{60} have been measured in the $h\nu$ range of 25–150 eV. The appearance photon energies are higher by 30–33 eV than the thermochemical thresholds for dissociative ionization of C_{60} leading to C_{60-2n}^{z+} + C_2. With increasing n the appearance energies shift to higher $h\nu$ positions for a given z. Evaluation is made on the upper limits of the internal energies of the primary C_{60}^{z+} above which $C_{60-2n+2}^{z+}$ fragments ($n \geq 1$) cannot escape from further dissociating into C_{60-2n}^{z+} + C_2. These upper limits agree well with the theoretical internal energies of C_{60}^{z+} corresponding to the threshold for the formation of C_{60-2n}^{z+}. The photofragmentation of C_{60}^{z+} is considered to be governed by the mechanism of internal conversion of the electronically excited states of C_{60}^{z+}, statistical redistribution of the excess energy among a number of vibrational modes, and successive ejection of the C_2 units.

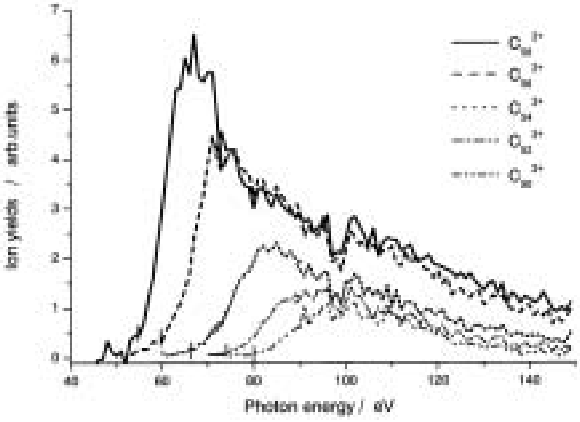

Figure 1. Yield curves of C_{60-2n}^{2+} ions (n = 1–5) obtained from time-of-flight mass spectra.

VI-I-6 Photoion Yields from Ce@C_{82} near the 4*d* Edge of Ce

MITSUKE, Koichiro; MORI, Takanori; KOU, Junkei; HARUYAMA, Yusuke[1]; KUBOZONO, Yoshihiro[1]
([1]Okayama Univ.)

The yield curves for photoions from Ce@C_{82} are measured by using synchrotron radiation in the photon energy range from 90 to 160 eV. Parent Ce@$C_{82}{}^{z+}$ and fragment ions $C_{60}{}^{z+}$ and $C_{70}{}^{z+}$ are observed in a mass spectrum (z = 1 and 2). The yield curves for principal ionic species exhibit broad resonance in the region $h\nu$ =120–140 eV which is ascribed to the $4d \rightarrow \varepsilon f$ giant dipole resonance of the encapsulated Ce atom. The total photoabsotpion cross section of Ce@C_{82} was determined from partial photofragmentation cross sections for respective ions to be $19.6^{+6.5}_{-3.9}$ and $5.3^{+1.8}_{-1.1}$ Mb at $h\nu$ = 110 and 130 eV, respectively.

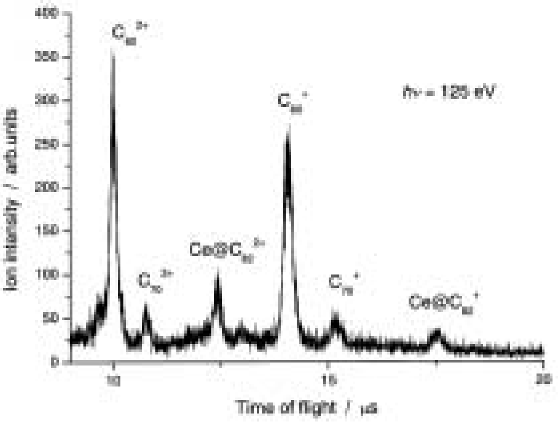

Figure 1. Time-of-flight mass spectrum of the parent and fragment ions produced by photoionization of Ce@C_{82} at $h\nu$ = 125 eV.